An unprecedented octahedral trifluoromagnesate $MgF_3(Wat)^-$ transition state analog reveals the molecular mechanism of ATP hydrolysis by Zika virus helicase

Mengyu Ge,[a] Robert W. Molt Jr.,[b,c] Huw T. Jenkins,[a] G. Michael Blackburn,[d] Yi Jin,[e*] and Alfred A. Antson[a*]

[a] York Structural Biology Laboratory, Department of Chemistry, University of York, York, YO10 5DD, United Kingdom

[b] Department of Biochemistry & Molecular Biology, Indiana University School of Medicine, Indianapolis, Indiana 46202, United States

[c] ENSCO, Inc., 4849 North Wickham Road, Melbourne, Florida 32940, United States

[d] Department of Molecular Biology and Biotechnology, University of Sheffield, Sheffield, S10 2TN, United Kingdom

[e] Cardiff Catalysis Institute, School of Chemistry, Cardiff University, Cardiff, CF10 3AT, United Kingdom

*Corresponding authors: JinY6@cardiff.ac.uk and fred.antson@york.ac.uk

Abstract: Metal fluoride complexes mimic the transferring phosphoryl group in many enzyme-catalyzed reactions. We here employ the trifluoromagnesate transition state analog (TSA) to study a Zika virus NS3h helicase, which uses energy from ATP hydrolysis to reorganize ssRNA leading to completion of virus replication. The crystal structure of this TSA complex displays two conformations for a catalytically important loop, demonstrating how ATP hydrolysis can be coupled with RNA translocation. Unexpectedly, the trifluoromagnesate core of this transition state complex is octahedral. It is identified as having an unprecedented $MgF_3(Wat)^-$ ligand, confirmed by ^{19}F NMR analysis. This structure was further probed by quantum mechanical calculations of the catalytic core (200 atoms), confirming the structural data interpretation and the concerted mechanism of ATP hydrolysis by this class of helicase. The formation of this $MgF_3(Wat)^-$ ligand in helicase but not in other multiple MF_x structures for ATPases and GTPases strongly implies they cannot possess such an additional water in their active sites.

Metal fluoride complexes have been immensely useful in studies of enzyme catalysis of phosphoryl group (PO_3^-) transfer. The tetrahedral BeF_3^- ground state analog (GSA) with octahedral AlF_4^- and trigonal bipyramidal (tbp) MgF_3^- transition state analog (TSA) complexes have enabled observation of molecular events that couple the catalytic steps of phosphoryl transfer to conformational changes.[1,2] Most of the structural information for molecular machines driven by ATP/GTP hydrolysis has been obtained by protein crystallography.[3,4] ^{19}F solution NMR has been equally important, complementing structural data with rigorous analysis of metal coordination. The combination of these experimental approaches has been particularly insightful for understanding catalytic mechanisms, and provides valuable data to support inhibitor design.[5]

Zika virus (ZIKV) is a positive-sense single-stranded RNA (ssRNA) virus. It is closely related to other members of the *Flaviviridae* family such as Dengue (DENV), Yellow Fever (YEV) and Hepatitis C (HCV) viruses (Figure S1). The global impact on health and economies from Zika infections has prompted extensive studies of its non-structural protein 3 (NS3).[6-8] NS3 contains an N-terminal protease and a C-terminal RNA helicase (NS3h) involved in RNA unwinding during viral replication.[9] NS3h has three domains (Figure S2),[10,11] with the interface between domains 1 and 2 forming a nucleotide triphosphate (NTP) binding pocket that comprises conserved catalytic Aspartate, Glutamate and Histidine.[12,13] As the energy derived from NTP hydrolysis allows the NS3 helicase to translocate along the leading strand of the nucleic acid, resulting in RNA unwinding, the NTP binding site is an attractive hotspot for antiviral drug design.

Considerable efforts have been made to obtain accurate structural data for molecular events associated with replication of *Flaviviridae* viruses focused on understanding the molecular basis of coupling between catalytic and mechanical cycles of motor proteins. Several crystallographic studies have examined ZIKV NS3h,[14-17] in particular, for substrate recognition based on complexes with ATP analogs,[14,15] ssRNA,[15] and also on the regulatory role of Mg^{2+}.[14] One of the general problems encountered by these researches has been distinguishing conformational changes induced by binding ssRNA, NTP and metal from conformational states clearly induced and stabilized by crystal packing forces. Furthermore, identification of subtle yet significant changes in bond lengths during catalysis has often been prevented by limited structural resolution.[17,18]

We first obtained an ADP trifluoroberyllate ground state complex structure for Zika virus NS3h at 1.7 Å resolution (Figure 1a, Table S1). The 1.7 Å resolution structure of NS3h-MnADP-BeF_3^- GSA complex was obtained by soaking Be^{2+} and F^- into NS3h-MnADP crystals to capture the pre-hydrolytic conformation of ATP with tetrahedral BeF_3^- (Figure 1a and 1d). In this structure, oxygen O^{W1} of the hydrolytic water molecule is 3.7 Å from Be^{2+}, donating an

anti-catalytic H-bond to F^1 (3.1 Å) and a second H-bond (2.8 Å) to the side-chain C=O of Q455 to give a near attack conformation (NAC).[1] The observed distances are somewhat longer than those seen in ssDNA-bound NS3h-MnADP-BeF_3^- complex for HCV, 3.5 Å (PDB 3KQU and 3KQN) to Be^{2+}, and 2.7 Å (PDB 3KQU) or 2.8 Å (PDB 3KQN) to the glutamine.[19] Thus our GSA complex structure suggests that polynucleotide binding tightens the pre-TS complex.

We then co-crystallized NS3h with ADP in the presence of 150 mM Mg^{2+} and 20 mM F^- and obtained the first high resolution structure for Zika NS3h in complex with magnesium trifluoride, determined at 1.50 Å resolution (Figure 1b, Table S1). Unexpectedly, the trifluoromagnesate moiety has octahedral geometry, in contrast to the generally observed tbp geometry.[4] This structure has clearly defined density for six-coordinate Mg^{2+} in the TSA ligand (Figure 1b). A square planar species located between the leaving group oxygen O^{3B} of ADP and the hydrolytic O^{W1} (Figure 1b and 1e) is defined in the omit electron density maps. The arrangement of this square planar moiety is very similar to that of AlF_4^- in the structure of a closely related homolog: HCV NS3h with ADP-AlF_4^- (PDB 3KQL and 5E4F).[18,19] We therefore further excluded potential contamination by AlF_4^- by adding deferoxamine, a strong aluminum chelator, to the crystallization solution.[20] The observed octahedral moiety with a central magnesium atom is unexpected since all 24 structures of trifluoromagnesate complexes (Table S4) in the PDB have five-coordinate MgF_3^- and are identified as isosteric TSAs for phosphoryl group in transfer.[21-23]

Examination of the omit map of this unusual complex shows weaker electron density at the position closest to R459 (Figure 1c and 1e), suggesting that the atom at this position is an oxygen. After fitting a water molecule (O^{MF}) into this position and fluorines in the other three equatorial positions, the Mg-F bond lengths refine to 1.88 Å and the Mg-O^{MF} bond length to 2.02 Å. They fall into the range of bond lengths of six-coordinated Mg,[24] while the axial O^{W1}-Mg-O^{3B} angle of NS3h-MgADP-$MgF_3(Wat)^-$ is 175.6° and the $\boldsymbol{r}_{DA}$ is 4.06 Å (Figure 1b). The distances from Mg^{2+} to O^{W1} and to the β-phosphate O^{3B} are 1.96 Å and 2.10 Å (Figure 1b), respectively. To our knowledge, $MgF_3(Wat)^-$ is a new TS mimic for the PO_3^- group, based on the dominant first-sphere coordination number of six for Mg^{II} while its unit negative charge makes it a more fitting TSA than either the dianionic MgF_4^{2-} or $MgF_3(OH)^{2-}$,[25] and supports the "priority of charge over geometry" concept for TSA complexes established for phosphoryl transfer enzymes.[20,26] This TSA complex locates E286 of NS3h as a general base to activate the nucleophilic water (Figure S3), similar to the conserved glutamate of DExx motif in other ATPases.[27,28]

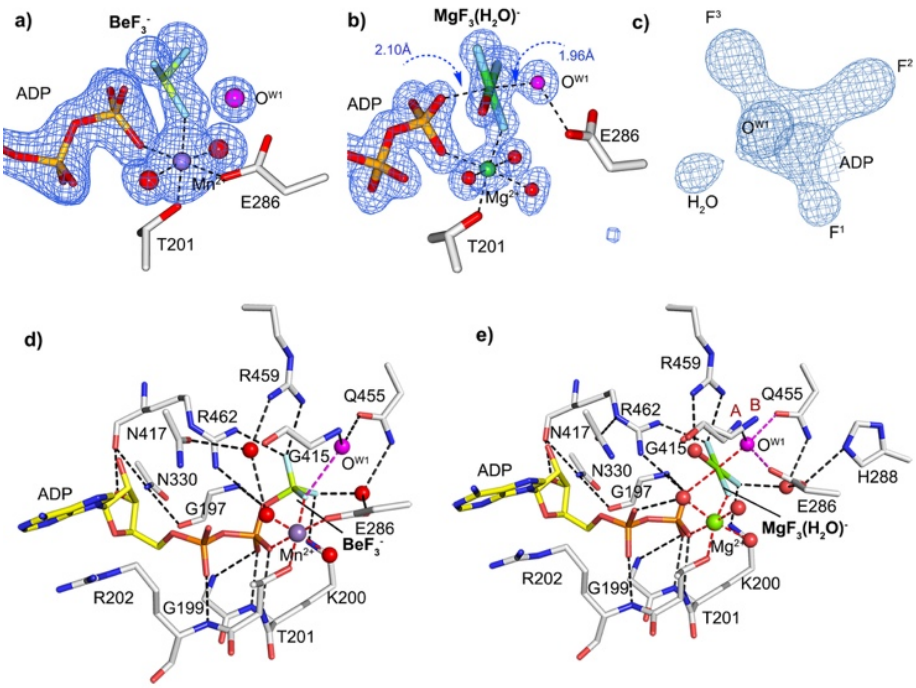

Figure 1. Comparison of transition state analog complex for the ZIKV NS3h-MgADP-MgF_3(Wat)$^-$ and ground state analog complex for NS3h-MnADP-BeF_3^-. a,b) Omit maps (mF_o-DF_c) of (a) ADP-BeF_3^- and (b) ADP-MgF_3(Wat)$^-$ complexes contoured at 4σ. c) Omit map of MgADP-MgF_3(Wat)$^-$ moiety, shown in different projection to (b) and contoured at 8σ. d,e) Active sites of (d) the NS3h-MnADP-BeF_3^- and (e) the NS3h-MgADP-MgF_3(Wat)$^-$ complexes. ADP carbon atoms are in yellow and protein carbon atoms are in silver. Water molecules are in red except for the nucleophilic water (W1) which is highlighted in magenta. Key differences in the W1 coordination are also in magenta. Beryllium is in lime; magnesium in green and fluorine in pale blue.

The single molecule of the NS3h in the asymmetric unit of the crystal, presents two conformations, A and B, for the conserved loop (Motif V) in the NS3h-MgADP-MgF_3(Wat)$^-$ structure (Figure 2). Conformation B adopts the usual "relaxed" position seen in the structures of NS3h-MnADP-BeF_3^- (Figure 2a), where the amide of G415 is 4.0 Å from the hydrolytic water O^{W1} and donates a H-bond (3.4 Å) to the backbone carbonyl of E413 (Figure 2b). In conformation A, following reorganization of the motif V loop, the amide of G415 moves 1.0 Å towards O^{W1} and donates a H-bond (3.0 Å) to coordinate it (Figure 2c). This shows conformation A is involved in ATP hydrolysis and does not require polynucleotide induction. Critically, the flexible conformation of the loop captured in the NS3h-MgADP-MgF_3(Wat)$^-$ crystal structure orientates the attacking water via tetrahedral coordination. Electron withdrawal from the O^{W1} by G415 is more than compensated by electron donation from $Q445_{(C=O)}$ and general base E286 to complete sp^3 orbital alignment with the O^{3B}-P^G antibonding orbital of ATP. Although this active site is relatively open compared to other NTPases (Figure S4), the tetrahedral coordination of the hydrolytic water prevents any

adventitious water from compromising its nucleophilicity. As Motif V is involved both in nucleic acid binding[19,29] and in TS formation (Figure 2, Table S3), it is likely that the conserved loop of this motif plays an important role in coupling NTP hydrolysis with RNA translocation.

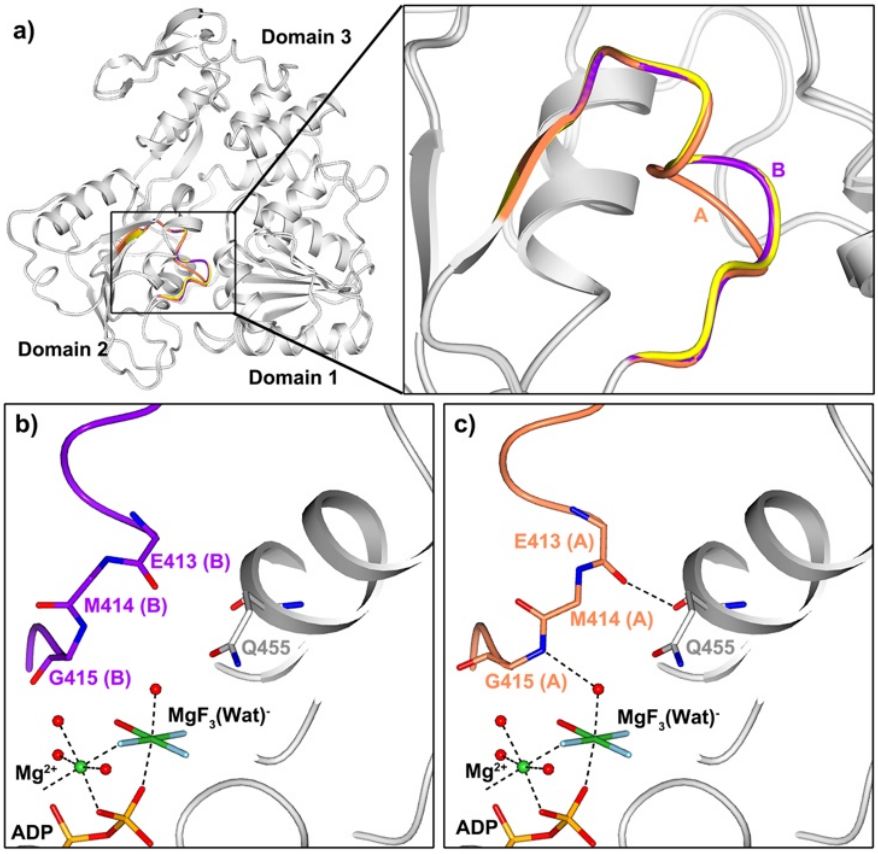

Figure 2. Two conformations of the conserved motif V loop in ZIKV NS3h. a) Superposition of NS3h-MgADP-$MgF_3(Wat)^-$ structure (light grey, conformation A in coral, conformation B in purple), and NS3h-MnADP-BeF_3^- (light grey, motif V loop in yellow). b,c) Side-by-side comparison of the two loop conformations in the NS3h-MgADP-$MgF_3(Wat)^-$ structure. Close-up views for the loop conformation B, magenta (b), and A, coral (c), are shown with Mg^{II} in green, fluorine in light blue, water molecules in red and H-bonds (≤ 3.1 Å) shown by dashed lines.

We examined the NS3h-MgADP-$MgF_3(Wat)^-$ complex by ^{19}F NMR to provide independent validation of the $MgF_3(Wat)^-$ moiety. As expected, the solution spectra showed three ^{19}F resonances present in 1:1:1 ratio (Figure 3), establishing that the magnesium fluoride moiety has only three fluorines, endorsing the crystal structure coordination. The observation of a single set of three fluorine resonances shows that the A and B conformations for the conserved loop are in fast exchange at 298 K. The three fluorines were assigned using solvent induced isotope shift (SIIS) values (Figure S5, Table 1), as SIIS accurately reflects the number and orientation of H-bond donors around each fluorine.[30] As for other phosphoryl transfer enzymes with catalytic Mg^{II}, F^1 (-175.2 ppm, SIIS 0.15 ppm) is the most shielded with weak H-bonding

interaction along with its coordination by magnesium. F^2 (-153.4 ppm; SIIS 1.44 ppm) is H-bonded to the side chain amino group of K200 and to a water molecule that is H-bonded to E286. F^3 is the most deshielded fluorine (-146.1 ppm; SIIS 1.38 ppm) with two H-bonds from the R459 and R462 guanidinium groups. These two arginines have been predicted to neutralize the negative charge developed on the *γ*-phosphate during ATP hydrolysis, acting like a "*trans*-arginine finger".[31] Replacing ATP by GTP gave unchanged ^{19}F spectra, demonstrating the absence of strict nucleotide specificity (Figure S6).

Octahedral AlF_4^- has been found to form a more stable complex than MgF_3^- for many phosphoryl transfer enzymes, having a much lower dissociation constant.[1,20,23,26,32,33] We therefore ran a competition experiment to investigate active site affinity of this unexplored $MgF_3(Wat)^-$ complex relative to AlF_4^-. Addition of 1 mM Al^{3+} to a sample of preformed NS3h-MgADP-$MgF_3(Wat)^-$ complex in the presence of 10 mM Mg^{2+}, resulted in a 5% decrease of the three ^{19}F resonances and the rise of a small, rotationally averaged peak at -152.1 ppm that is Al^{III} associated, showing 5% of the active site switched from $MgF_3(Wat)^-$ to tetrafluoroaluminate. Addition of Al^{3+} to 5 mM final concentration, gives only 50% conversion of $MgF_3(Wat)^-$ into AlF_4^- (Figure 3a). This limited conversion to AlF_4^- further demonstrates that $MgF_3(Wat)^-$ has NS3h TSA stability at least equivalent to that of AlF_4^-, since an AlF_4^- complex would achieve full-occupancy only at a higher concentration of Al^{3+} (at least 20 mM).

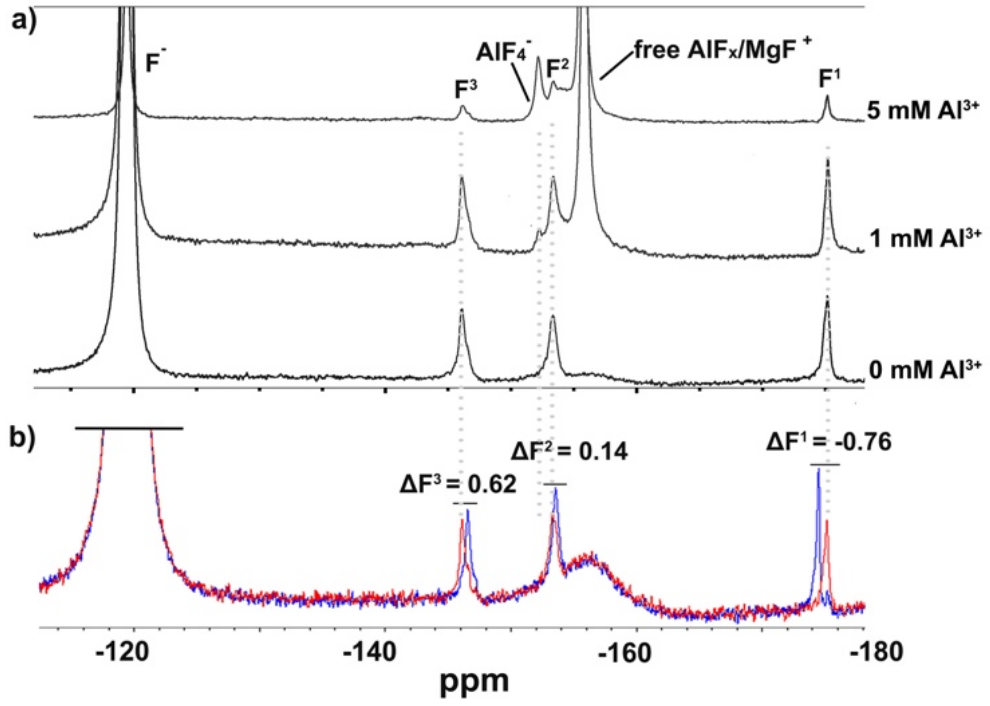

Figure 3. ^{19}F NMR spectra of ZIKV NS3h-MgADP-$MgF_3(Wat)^-$ TSA complexes. a) ^{19}F NMR spectra of the Al^{3+} titration to convert NS3h-MgADP-$MgF_3(Wat)^-$ (F^3 = -146.12 ppm, F^2 = -153.36 ppm, F^3 = -175.16

ppm) into NS3h-MgADP-AlF_4^- complexes in 90% H_2O buffer. Following addition of 1 mM $AlCl_3$ or 5 mM $AlCl_3$, the 152.10 ppm chemical shift of bound AlF_4^- was observed as a rotationally averaging peak. b) ^{19}F NMR spectra of ssRNA-free (red, F^3 = -146.12 ppm, F^2 = -153.36 ppm, F^1 = -175.16 ppm) and ssRNA-bound (blue, F^3 = -146.59 ppm, F^2 = -153.58 ppm, F^1 = -174.48 ppm) NS3h-MgADP-$MgF_3(Wat)^-$ TSA complexes. Chemical shift differences for each resonance are shown.

While attempts to crystallize an ssRNA-bound TSA complex were unsuccessful, we were able to investigate conformational changes induced by ssRNA binding using solution ^{19}F NMR. When ssRNA was added to the sample of NS3h-MgADP-$MgF_3(Wat)^-$ TSA complex, the three fluorine resonances in the ^{19}F NMR changed only by 0.62 ppm for F^3, 0.14 ppm for F^2, and -0.76 ppm for F^1 (Figure 3b). This indicates only a small difference of the H-bonding network within the NS3h catalytic site and subtle conformational changes upon ssRNA binding. Notably all three fluorine resonances of the $MgF_3(Wat)^-$ complex increase in intensity by ~20% upon addition of ssRNA, most prominently for F^1 (Figure 3b). This suggests that binding of ssRNA retards exchange between $MgF_3(Wat)^-$ TSA moiety and free MgF_x resulting from tighter binding of the TSA complex. Likewise, a doubling of K_D for ADP-AlF_4^- in the absence of ssDNA has been observed for the HCV NS3h by fluorescence polarization.[17] Binding ssRNA also slightly increases the SIIS values for all three fluorines, consistent with overall H-bond shortening in the TSA complex (Table 1). It is clear that ^{19}F NMR provides direct evidence for ssRNA-stimulated NTPase activity indicating conformational closure of the finely-tuned H-bond network around the transferring phosphoryl group in the TS, as observed for HCV NS3h.[18] These ^{19}F NMR observations thus provide the first experimental data on the NS3h complexes in TS conformation both in the presence and absence of a polynucleotide in solution.

Table 1. Solvent induced isotope shifts (SIIS, ppm) for ^{19}F NMR signal of RNA-free and RNA-bound ZIKV NS3h-ADP-$MgF_3(Wat)^-$ complex.

NS3h-MgADP-$MgF_3(Wat)^-$ [a]		**F^3**	**F^2**	**F^1**
RNA-bound	$\delta^{19}F_{(90\%H2O)}$	-146.59	-153.58	-174.48
	SIIS	1.40	1.50	0.20
RNA-free	$\delta^{19}F_{(90\%H2O)}$	-146.12	-153.36	-175.16
	SIIS	1.38	1.44	0.15

[a] SIIS = $\delta\ ^{19}F_{\ (90\%\ H2O\ buffer)} - \delta\ ^{19}F_{\ (100\%\ D2O\ buffer)}$.

Lastly, we have analyzed the TSA core using density functional theory (DFT) first to validate the assignment of the ligand as $MgF_3(Wat)^-$ and then to determine the true TS for phosphoryl transfer in the hydrolysis of ATP. We selected segments from 18 amino acids, MeDP (methyl diphosphate) representing ADP, and $MgF_3^-(Wat)$-H_2O for the QM zone, a total of 108 non-hydrogen atoms (Figure 4). Fifteen carbons at the periphery for both conformations A and B were 'locked' onto the coordinates of the crystal structure for NS3h-MgADP-$MgF_3(Wat)^-$ (see SI).[2,34] To test the "charge over geometry" hypothesis, both OH^- and H_2O were fitted to the position of Wat, but only H_2O maintained the observed octahedral structure seen in the crystal structure. Also, H288 was computed in both its neutral and protonated form in DFT analyses, but only the neutral H288 delivered the orientation of E286 observed in the crystal structure. The computed NS3h-MeDP-$MgF_3(Wat)^-$ structures for the A and B conformations show excellent agreement with the crystal structure (RMSD 0.30 and 0.40 Å, respectively) (Figure S7a). The network of core H-bonds is well reproduced with $MgF_3(Wat)^-$ accepting 6 H-bonds from R459 (2 bonds), R462, K200, W168 and W331, and also coordinating Mg_{cat}^{2+}, thus validating the assignment of the electron density to $MgF_3^-(Wat)$ (Figure S7b). In particular, Wat donates a H-bond to the π–cloud of R459 guanidinium.[34] The TS for basal ATP catalysis by NS3h was computed after replacing the $MgF_3(Wat)^-$ core by the trigonal planar PO_3^- group with a water molecule taking the position of O^{MF} in the initial geometry (Figure 4b). Vibrational frequency analysis showed that a reliable TS geometry has been achieved for both conformations, A and B (Movies S1), visualizing general base catalysis in the TS. Comparing the calculated phosphoryl TS of conformation A with the observed TSA structures, the only major difference is the angular increase from 118° for O^{1G}-P-O^{3G} to 179° for F^1-Mg-F^3, to enable water to coordinate the surrogate magnesium in the octahedral complex (Figure S8).

Over 200 metal fluoride complexes have been characterized for ATPases and GTPases in combination with a NDP but an octahedral $MgF_3(Wat)^-$ has not been identified hitherto.[3,4] This raises two questions: "How is this species formed in helicase" and "Why has it not been isolated in other metal fluoride structures before?" The answer the first problem is provided from two sources. First, our ADP-BeF3 complex (PDB 6RWZ) and a well-resolved structure (PDB 5Y6N; 1.57 Å) of the Zika virus NS3h with ADP bound both have an additional water in the same location as seen in the $MgF_3(Wat)^-$ complex with identical coordination to R459-NH1 and Mg_{cat}-bonded Wat846.[17] Secondly, our DFT-computed TS for NS3h ATP hydrolysis shows the water in the $MgF_3(Wat)^-$ complex is liberated in the PO_3^- TS, moving 1.5 Å further from PG (Figure 4a,b). It remains coordinated to Arg459 and Wat846 with a new H-bond to O3G (Figure 4c). Its oxygen lies in the plane of the transferring phosphoryl group, 4.3 Å from the nucleophilic water. Thus, it can play only a minor role in the reaction mechanism. We conclude that when MgF_3^- is generated within a catalytic complex as a mimic of PO_3^- and locates an

isolated, proximate water, its coordination shell expands from tbp to octahedral geometry to generate a complex of greater stability with this water as its sixth ligand.

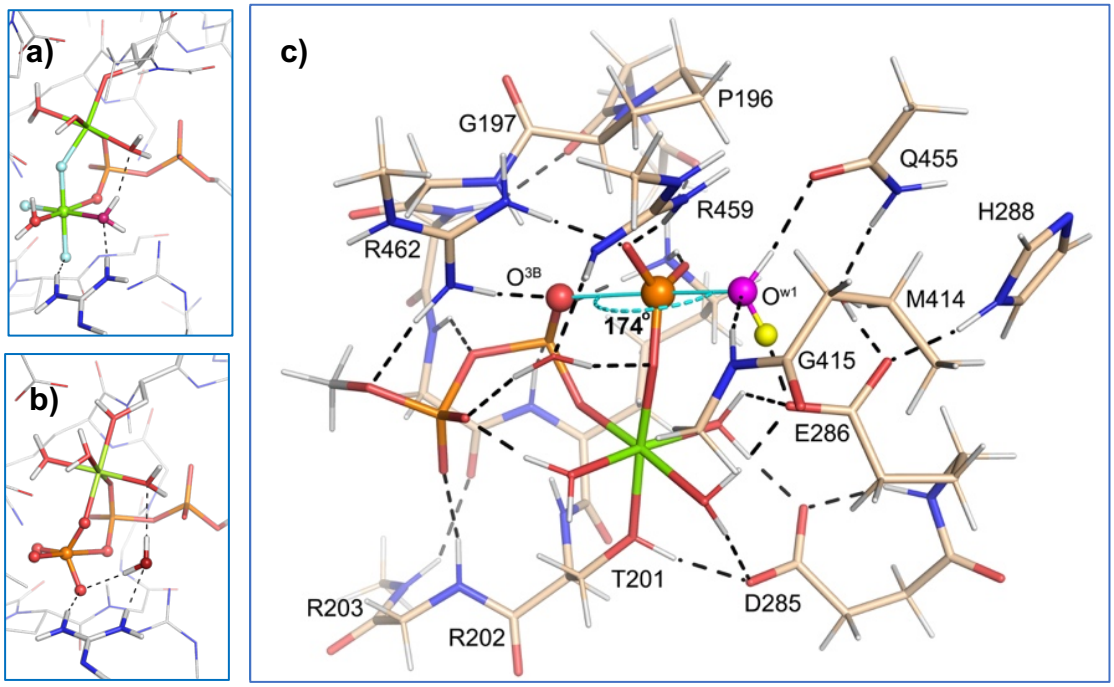

Figure 4. Comparison of water molecule "Wat" in a) TSA complex for the ZIKV NS3h-MgADP-$MgF_3(Wat)^-$ and b) computed TS for ZIKV NS3h ATP hydrolysis. c) Computed TS for ATP hydrolysis showing contributions of 18 amino acids to the 23 H-bond network in the catalytic complex embracing MgATP (108 total atoms). The donor O^{3B} (red sphere) and acceptor O^{w1} (magenta sphere) oxygens for P^G (orange sphere) are highlighted, as is the proton (yellow sphere) transferring from O^{w1} to E286 (carbon, eggshell; hydrogen, white; nitrogen, blue; oxygen, red; phosphorus, orange; magnesium, pale green).

The answer to the first question now bears directly on the second question. There are some 70 MF_x tbp TSA complexes of ATPases and GTPases.[3,4] Were any of these to have a proximate, unliganded water within its catalytic TSA complex, the trigonal bipyramidal MF_3 complex would transform spontaneously into a more-stable, octahedral $MgF_3(Wat)^-$ complex. The singularity of our helicase $MgF_3(Wat)^-$ TSA complex clearly signals the absence of a second water in all tbp MF_x TSA structures yet examined. This conclusion fully endorses our analysis of the requirement of water exclusion from the catalytic sites of other ATPase and GTPase enzymes which would compromise the tight H-bonding architecture essential for activation of the isolated nucleophilic water to attack PG.[3,4] It conflicts directly with the hypothesis of "a second water as a necessary catalytic component for GTP hydrolysis by small G proteins" that has been used as the basis of some computational modelling studies[3,4,34,36].

This hypothesis has proved very controversial, not least because no second water has been observed in any structure of a TS complex for phosphoryl transfer.[3,4] The support for this proposal is solely based on a 2.5 Å structure of a "Ras-GDP-AlF_3^0 complex" (PDB: 1WQ1) that has no observation of the density of a second water. The discovery of our $MgF_3(Wat)^-$ complex now strongly challenges the structural assumption underlying these computations.

The close agreement between spectroscopic, structural, and computational studies on ZIKV NS3 helicase enables a rigorous analysis of the atomic details of the conformational switch between the ssRNA-free and ssRNA-bound states, which is central to the function of NS3h during replication of ZIKV. The clear distinction between the RNA-free and RNA-bound TSA complexes is manifested in subtle yet significant differences in H-bonding (Figure 3b). The conserved loop from motif V adopts two conformations in the TSA NS3h-MgADP-$MgF_3(Wat)^-$ complex structure. Significantly, conformation A has not been previously observed in nucleic acid-free TSA complex structures of NS3 helicases of *Flaviviridae* viruses (Table S3). The two conformations adopted by the catalytically important loop (motif V), in the presence of the $MgF_3(Wat)^-$ TSA demonstrate how ATP hydrolysis affects protein conformation. While motif V has been known to be responsible for nucleic acid binding in other flaviviridae NS3h,[19,37] our results illuminate how ATP hydrolysis links with mechanical translocation of RNA. The previously unobserved structure of the $MgF_3(Wat)^-$ transition state analog, reported here, could be more widely existing and used successfully to study the mechanism of other enzymes involving NTP hydrolysis that have active sites more open to solvation by additional water.

Experimental Section

Crystallographic data, structure determination and refinement statistics, raw NMR data as well as details of the computational analysis are provided in the Supplementary Information. Structural data for the NS3h-MgADP-$MgF_3(Wat)^-$ TSA and NS3h-MnADP-BeF_3^- GSA complexes have been deposited with the Protein Data Bank under accession codes **6S0J** and **6RWZ,** respectively.

Acknowledgements

We thank S. Hart and Dr. J. Turkenburg from York Structural Biology Laboratory for data collection and Diamond Light Source for the access to beamline I02 and I03 (proposal number mx13587), and Dr. M. J. Cliff from Manchester Institute of Biotechnology for assistance with ^{19}F NMR data. We thank Indiana University for access to the Big Red 2 supercomputer and Lilly Endowment, Inc. for support of the Indiana University Pervasive Technology Institute and the Indiana METACyt Initiative. We thank the Wellcome Trust WT098230 and WT101528

funding to AAA; China Scholarship Council Award 201506320181 and Wild Fund studentship to MG.

Conflict of interest

The authors declare no conflict of interest.

Keywords: Zika virus helicase • Transition State Analog • ATPase • Bio-^{19}F NMR • Protein Crystallography • General base catalysis • Phosphoryl transfer mechanism

References

1. Jin, Y., Molt, R. W., Waltho, J. P., Richards, N. G. J. & Blackburn, G. M. ^{19}F NMR and DFT Analysis Reveal Structural and Electronic Transition State Features for RhoA-Catalyzed GTP Hydrolysis. *Angew. Chemie - Int. Ed.* **55**, 3318–3322 (2016).
2. Jin, Y. *et al.* Assessing the Influence of Mutation on GTPase Transition States by Using X-ray Crystallography,^{19}F NMR, and DFT Approaches. *Angew. Chemie - Int. Ed.* **56**, 9732–9735 (2017).
3. Jin, Y., Molt, R. W. & Blackburn, G. M. Metal Fluorides: Tools for Structural and Computational Analysis of Phosphoryl Transfer Enzymes. *Top. Curr. Chem.* **375**, 1–31 (2017).
4. Jin, Y., Richards, N. G., Waltho, J. P., & Blackburn, G. M. (2017). Metal fluorides as analogues for studies on phosphoryl transfer enzymes. *Angew. Chem. - Int. Ed*, **56**, 4110-4128 (2017).
5. Schramm, V. L. Transition states, analogues, and drug development. *ACS Chem. Biol.* **8**, 71–81 (2013).
6. Slavov, S. N., Otaguiri, K. K., Kashima, S. & Covas, D. T. Overview of Zika virus (ZIKV) infection in regards to the Brazilian epidemic. *Brazilian J. Med. Biol. Res.* **49**, 1–11 (2016).
7. Neufeldt, C. J., Cortese, M., Acosta, E. G. & Bartenschlager, R. Rewiring cellular networks by members of the Flaviviridae family. *Nat. Rev. Microbiol.* **16**, 125–142 (2018).
8. Klema, V. J., Padmanabhan, R. & Choi, K. H. Flaviviral replication complex: Coordination between RNA synthesis and 5'-RNA capping. *Viruses* **7**, 4640–4656 (2015).
9. Pérez-Villa, A., Darvas, M. & Bussi, G. ATP dependent NS3 helicase interaction with RNA: Insights from molecular simulations. *Nucleic Acids Res.* **43**, 8725–8734 (2015).

10. Cox, B. D., Stanton, R. A. & Schinazi, R. F. Predicting Zika virus structural biology: Challenges and opportunities for intervention. *Antivir. Chem. Chemother.* **24**, 118–126 (2015).

11. Rice, C. M. *et al.* Nucleotide sequence of yellow fever virus: Implications for flavivirus gene expression and evolution. *Science* **229**, 726–733 (1985).

12. Gorbalenya, A. E. & Koonin, E. V. Helicases: amino acid sequence comparisons and structure-function relationships. *Curr. Opin. Struct. Biol.* **3**, 419–429 (1993).

13. Singleton, M. R., Dillingham, M. S. & Wigley, D. B. Structure and Mechanism of Helicases and Nucleic Acid Translocases. *Annu. Rev. Biochem.* **76**, 23–50 (2007).

14. Cao, X. *et al.* Molecular mechanism of divalent-metal-induced activation of NS3 helicase and insights into Zika virus inhibitor design. *Nucleic Acids Res.* **44**, 10505–10514 (2016).

15. Tian, H. *et al.* Structural basis of Zika virus helicase in recognizing its substrates. *Protein Cell* **7**, 562–570 (2016).

16. Jain, R., Coloma, J., García-Sastre, A. & Aggarwal, A. K. Structure of the NS3 helicase from Zika virus. *Nat. Struct. Mol. Biol.* **23**, 752–754 (2016).

17. Yang, X. *et al.* Mechanism of ATP hydrolysis by the Zika virus helicase. *FASEB J.* **32**, 5250–5257 (2018).

18. Gu, M. & Rice, C. M. The spring α-helix coordinates multiple modes of HCV (hepatitis C virus) NS3 helicase action. *J. Biol. Chem.* **291**, 14499–14509 (2016).

19. Gu, M. & Rice, C. M. Three conformational snapshots of the hepatitis C virus NS3 helicase reveal a ratchet translocation mechanism. *Proc. Natl. Acad. Sci.* **107**, 521–528 (2010).

20. Jin, Y. *et al.* Charge-balanced metal fluoride complexes for protein kinase A with adenosine diphosphate and substrate peptide SP20. *Angew. Chemie - Int. Ed.* **51**, 12242–12245 (2012).

21. Graham, D. L. *et al.* MgF_3^- as a transition state analog of phosphoryl transfer. *Chem. Biol.* **9**, 375–381 (2002).

22. Baxter, N. J. *et al.* A Trojan horse transition state analogue generated by MgF_3^- formation in an enzyme active site. *Proc. Natl. Acad. Sci.* **103**, 14732–14737 (2006).

23. Jin, Y. *et al.* Fluorophosphonates reveal how a phosphomutase conserves transition state conformation over hexose recognition in its two-step reaction. *Proc. Natl. Acad. Sci.* **111**, 12384–12389 (2014).

24. Bock, C. W., Kaufman, A. & Glusker, J. P. Coordination of water to magnesium cations. *Inorg. Chem.* **33**, 419–427 (1994).

25. Bock, C. W., Katz, A. K., Markham, G. D. & Glusker, J. P. Manganese as a replacement for magnesium and zinc: Functional comparison of the divalent ions. *J. Am. Chem. Soc.* **121**, 7360–7372 (1999).

26. Baxter, N. J. *et al.* Anionic charge is prioritized over geometry in aluminum and magnesium fluoride transition state analogs of phosphoryl transfer enzymes. *J. Am. Chem. Soc.* **139**, 3952–3958 (2008).

27. Zhang, X. & Wigley, D. B. The 'glutamate switch' provides a link between ATPase activity and ligand binding in AAA+ proteins. *Nat. Struct. Mol. Biol.* **15**, 1223–1227 (2008).

28. Lee, J. Y. & Yang, W. UvrD Helicase unwinds DNA one base pair at a time by a two-part power stroke. *Cell* **127**, 1349–1360 (2006).

29. Luo, D. *et al.* Insights into RNA unwinding and ATP hydrolysis by the flavivirus NS3 protein. *EMBO J.* **27**, 3209–3219 (2008).

30. Hansen, P. E., Dettman, H. D. & Sykes, B. D. Solvent-induced deuterium isotope effects on19F chemical shifts of some substituted fluorobenzenes. Formation of inclusion complexes. *J. Magn. Reson.* **62**, 487–496 (1985).

31. Sampath, A. *et al.* Structure-Based Mutational Analysis of the NS3 Helicase from Dengue Virus. *J. Virol.* **80**, 6686–6690 (2006).

32. Cliff, M. J. *et al.* Transition state analogue structures of human phosphoglycerate kinase establish the importance of charge balance in catalysis. *J. Am. Chem. Soc.* **132**, 6507–6516 (2010).

33. Liu, X. *et al.* Prioritization of charge over geometry in transition state analogues of a dual specificity protein kinase. *J. Am. Chem. Soc.* **133**, 3989–3994 (2011).

34 Kamerlin, S. C., Sharma, P. K., Prasad, R. B. & Warshel, A. Why nature really chose phosphate. *Quart. Revs. Biophys.* **46**, 1-132 (2013).

35. Siegbahn, P. E. & Borowski, T. Comparison of QM-only and QM/MM models for the mechanism of tyrosinase. *Faraday Discuss* **8**, 3793–3803 (2011).

36. Hoepfner, V., Deringer, V. L. & Dronskowski, R. Hydrogen-bonding networks from first-principles: exploring the guanidine crystal. *J. Phys. Chem. A* **116**, 4551–4559 (2012).

37. Myong, S., Bruno, M. M., Pyle, A. M. & Ha, T. Spring-loaded mechanism of DNA unwinding by hepatitis C virus NS3 helicase. *Science* **317**, 513–516 (2007).